

PULL-OUT CAPACITIES OF SCREW CONNECTIONS IN CFS CLADDING SYSTEMS UNDER COMBINED WIND AND BUSHFIRE ACTIONS

G. Athmarajah*, M. Mahendran* and A. Ariyanayagam**

* PhD researcher and Professor

e-mails: gopikrishna.athmarajah@hdr.qut.edu.au, m.mahendran@qut.edu.au

** Senior lecturer

e-mail: a.ariyanayagam@qut.edu.au

Keywords: Cold-formed steel cladding systems; Steel battens; Screw connections; Pull-out failures; Bushfires; Wind loading; Elevated temperatures.

Abstract. Cold-formed steel (CFS) roof and wall cladding systems are popular globally, especially in bushfire-prone regions due to their non-combustible properties. Australian Standard AS 3959 recommends their use in such areas. To protect buildings from embers during bushfires, the external envelope must remain undamaged with gaps less than 2 mm. However, wind and bushfire interactions can cause localised failures in thin steel cladding systems at screw connections. The behavior of CFS steel cladding and batten screw connections under elevated temperatures is not well understood. This study aims to investigate the pull-out failure behavior and capacities of such connections under wind uplift and elevated temperatures. 216 small-scale tests were conducted on different CFS batten thicknesses and strengths, using various screw fasteners. The results will lead to design rules and reduction factors for safer building construction in bushfire-prone areas, potentially preventing future.

1 INTRODUCTION

Environmental conditions create catastrophes that result in bushfires. Australians are particularly vulnerable to them due to their high fire prone nature, which causes severe damage to living organisms and assets globally [1]. There is an increased risk of damage to existing infrastructure caused by strong winds. It is possible for structures like roofs to be dislodged due to the interaction between fire and wind during bushfires. The interaction between fire and wind has been demonstrated to dramatically increase the wind pressure and suction near buildings through computational fluid dynamics simulations [2-5]. Wind pressures are possible to cause considerable damage to a building even before a bushfire directly impacts it. The Black Summer bushfires in Australia were also characterized by pyro-convective atmospheric events such as fire tornadoes, which were witnessed during the 2019-2020 bushfire season. Deaths, home destruction, and extensive vertebrate loss resulted from these fires [6]. Kangaroo Island and Jingellic experienced bushfire-enhanced wind events, including fire tornadoes during that period (figure 1). Australian standard AS3959 [7] specifies three mechanisms for bushfire attack: flame contact, radiant heat, and ember attack. These mechanisms are merely indicators of bushfire attack. For communities and structures to survive such disasters, a comprehensive understanding of bushfire-generated wind is crucial. To prevent ember ingress, AS 3959 and NASH [8] recommend a 2mm gap in bushfire-prone areas. Because of their non-combustibility, CFS cladding systems with thin and high strength claddings and battens are frequently used in bushfire-prone places (figure 2). As a result of bushfire-induced winds in previous incidents, the cladding on roofs and walls failed. During bushfires, roofs and walls must be protected.

The pull-out failures of screw connections with sheeting and CFS battens are more prevalent, thus this paper focuses on them. The pull-out capacities and failures of different screw fastener systems in CFS structures have been explored including static and cyclic pull-out failures, clip angles, C-shaped connectors [9-15]. Moreover, screw connections to CFS structures at elevated temperatures were also tested to examine shear failure mechanisms [16-19]. In addition, several researchers performed elevated mechanical properties experiments [20-25]. CFS batten pull-out failure loads at elevated temperatures are studied in this paper. A capacity reduction factor and design equations will be developed to determine batten pull-out in such conditions.



Figure 1: Fire tornado at Thargomindah, Queensland [26]

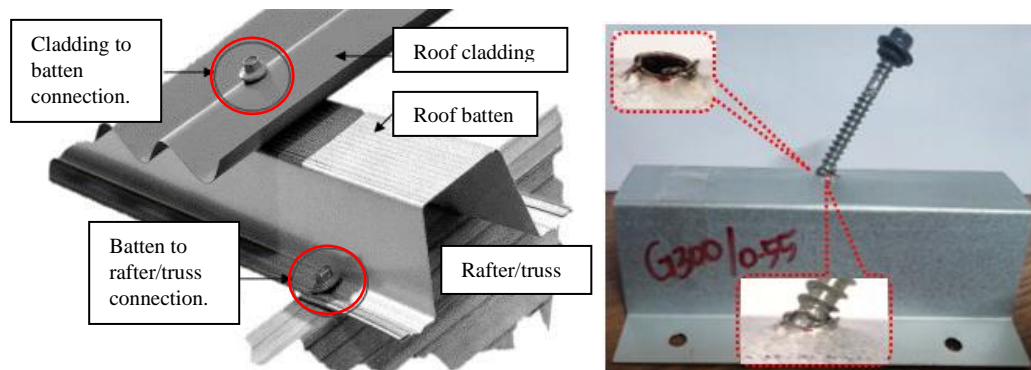


Figure 2: Typical CFS roof structures [27] and pull-out failure.

2 EXPERIMENTAL STUDY

2.1 Test specimen

Pull-out failures were predicted by testing 150mm long CFS battens with screws at elevated temperatures. Bending forces have a minimal effect on pull-out failures [10]. A shorter batten was used following European and American standards, with specimens being minimum 100mm long [28, 29]. Batten thickness, ultimate strength of batten steel, and screw thread characteristics significantly affected pull-out failures [10]. The common thicknesses for battens in Australia are 0.55mm, 0.75mm, and 0.80mm. Steel battens G550 were the only commercially available, but G300 were fabricated for testing. TS 4055, TS 4075, and QUT-made battens with specific geometric profiles were used in this experiment. Tek, Zip, and T17 screw types were used for fixing cladding to battens. Experiments were conducted on specific screws of each type and are given in table 1 (figure 3). 216 tests were conducted at 20 °C to 600 °C, with three repetitions for accuracy [30]. G550, 0.55, 10g-16 and # represent batten steel grade, batten thickness in mm, screw fastener and temperature, respectively, in Table 1 under the name column.

Table 1: Details of screw fasteners.

Screw fastener group	Screws	TPI	p (mm)	d (mm)	d ₁ (mm)	DD (mm)
Zips	M6-11	11	2.31	6.00	4.20	3.10
Teks	10g-16	16	1.59	4.73	3.51	3.85
T17	12g-11	11	2.31	5.60	4.07	0.00

TPI – threads per inch, p – pitch, d- thread outer diameter, d₁ – thread inner diameter and DD – thread drill point diameter.

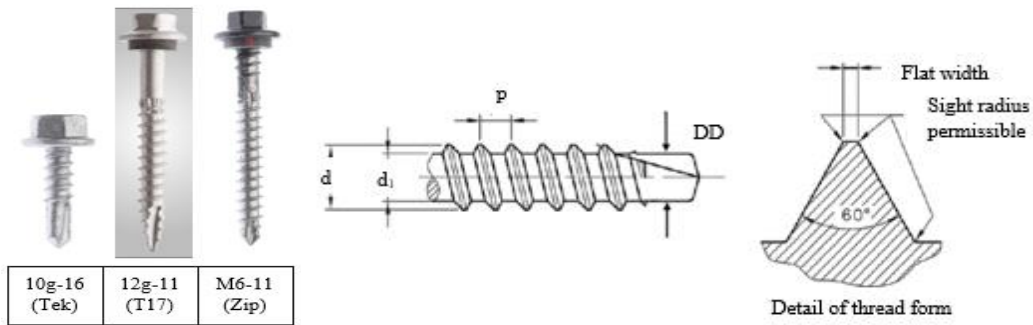


Figure 3: Screw fasteners and thread details [31]

Table 2: Test plan of pull-out failure at elevated temperatures.

Name	Temperature (°C)	No. of tests
G550_0.55_10g-16_#	20, 200, 300, 400, 500, 600	18
G550_0.75_10g-16_#	20, 200, 300, 400, 500, 600	18
G300_0.55_10g-16_#	20, 200, 300, 400, 500, 600	18
G300_0.80_10g-16_#	20, 200, 300, 400, 500, 600	18
G550_0.55_12g-11_#	20, 200, 300, 400, 500, 600	18
G550_0.75_12g-11_#	20, 200, 300, 400, 500, 600	18
G300_0.55_12g-11_#	20, 200, 300, 400, 500, 600	18
G300_0.80_12g-11_#	20, 200, 300, 400, 500, 600	18
G550_0.55_M6-11_#	20, 200, 300, 400, 500, 600	18
G550_0.75_M6-11_#	20, 200, 300, 400, 500, 600	18
G300_0.55_M6-11_#	20, 200, 300, 400, 500, 600	18
G300_0.80_M6-11_#	20, 200, 300, 400, 500, 600	18

2.2 Test setup

An elevated testing setup is shown in Figure 4 to predict the pull-out failure loads of screw connections. An electric furnace, displacement gauges (LVDTs), 10 kN load cells, hydraulic pumps, and a data acquisition controller (UDAQ) are included in the setup. K-type thermocouples were attached to the top flange to measure the batten's temperature. An enclosed M20 nut was used to attach screw fasteners to the batten's top flange. The batten was mounted upside down via Unbrako bolts and nuts. The flat plate was placed into the test rig and a steel pin was used to connect the loading rod and bottom shaft fixed with loading cell. An electric furnace door was closed after assembling thermocouples on the top flange. UDAQ was setup

to accurately record measurements from load cells, LVDTs, and thermocouples before the experiments started. UDAQ recorded the tensile forces and vertical displacements of screw fasteners via load cells and LVDTs. Before testing, displacements and loads were recalibrated to zero. Setting the target temperature on the Eurotherm controller initiated the heating process. Upon reaching the target temperature, the battens were kept at the same temperature for 10 minutes. The specimens were then loaded downward by a hydraulic pump. The experiments continued until the load dropped significantly.

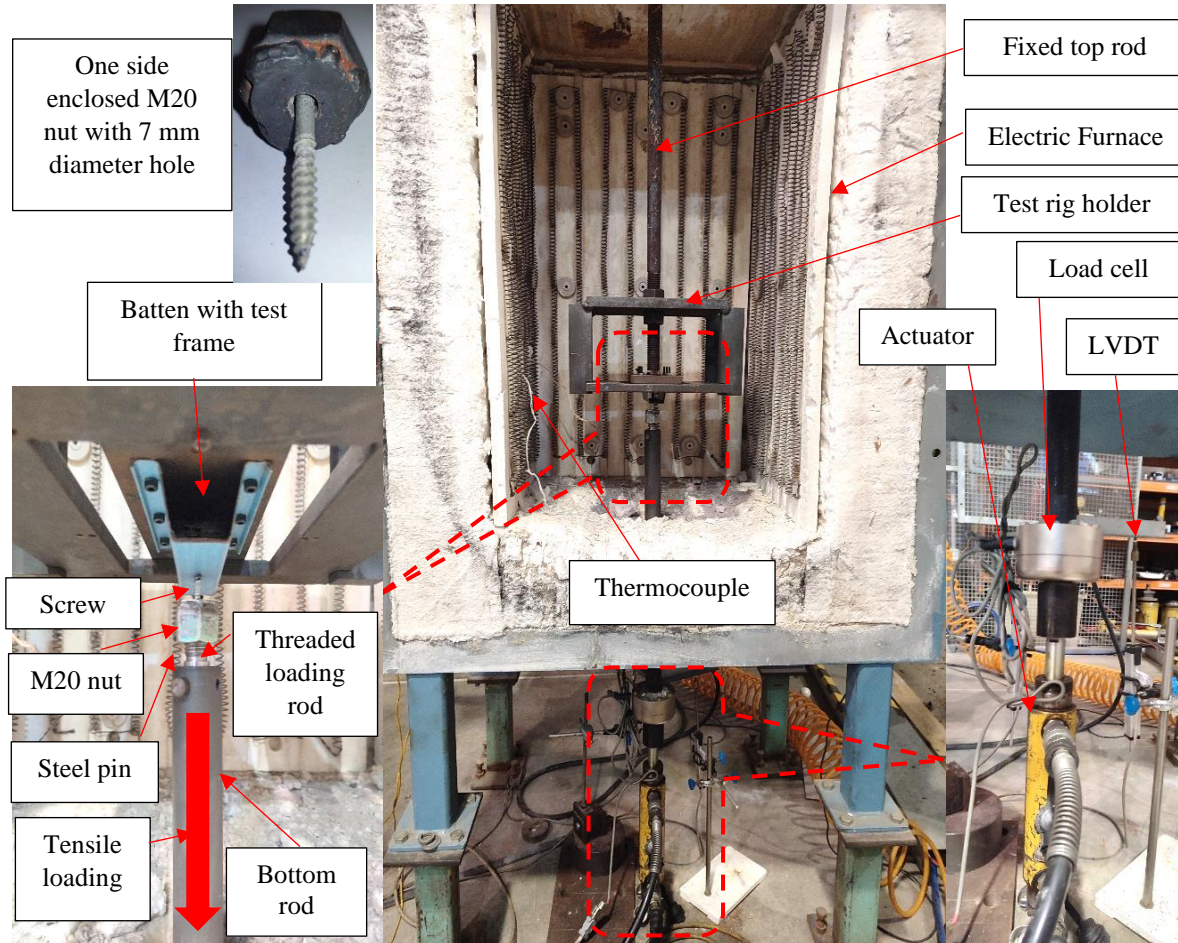


Figure 4: Short batten test arrangement.

3 TEST RESULTS AND DISCUSSION

3.1 Validation of test setup

Batten pull-out capacities at ambient temperatures can be determined using two design equations independently developed in Australia [9, 10]. A more recent design rule by Sivapathasundaram and Mahendran [10] incorporated results from Mahendran and Tang [9]. The accuracy of the testing setup inside the electric furnace was evaluated by comparing Sivapathasundaram and Mahendran's equation ($P_{u, SM}$) with experimental results from this study ($P_{u, test}$). There was an acceptable COV limit for $P_{u, test} / P_{u, SM}$, with a mean value of 0.98 as given in table 3. Test setup can provide reliable predictions for failure loads on battens at elevated temperatures.

3.2 Failure modes

Based on steel thickness vs. thread pitch, pull-out failures on battens showed permanent bending deformations and failures without noticeable deformations. Permanent deformation failures occurred when the steel thickness was thinner than the thread pitch. Minimum pitch of 1.59 mm (10g-16 screw) and a maximum batten thickness (0.80mm) of this research resulted in permanent bending deformations. In spite of batten configurations and elevated temperatures, these failure modes persisted (figure 5). At ambient temperatures, permanent bending deformations have also been observed. Load-displacement graphs of different batten configurations under pull-out at elevated temperatures were presented in figure 6.



Figure 5: Permanent deformations on battens during pull-out

Table 3: Comparison of mean batten pull-out failure loads at ambient temperature.

Specimen	$P_{u, test}$ (N)	$P_{u, SM}$ (N)	$P_{u, test}$ / $P_{u, SM}$
G550_0.55_10g-16_20	1126	1156	0.97
G550_0.75_10g-16_20	1694	1611	1.05
G550_0.55_12g-11_20	1436	1373	1.05
G550_0.75_12g-11_20	1993	1914	1.04
G550_0.55_M6-11_20	1412	1513	0.93
G550_0.75_M6-11_20	2091	2109	0.99
G300_0.55_10g-16_20	718	808	0.89
G300_0.80_10g-16_20	1148	1305	0.88
G300_0.55_12g-11_20	1105	960	1.15
G300_0.80_12g-11_20	1428	1550	0.92
G300_0.55_M6-11_20	974	1058	0.92
G300_0.80_M6-11_20	1557	1708	0.91
		Mean	0.98
		COV	0.08

4 DEVELOPMENT OF DESIGN EQUATIONS

4.1 Overview of existing design equations

The pull-out capacity design equations given in AS/NZS 4600:2018 (equation (1)), AISI S100:2012 (equation (2)), and Eurocode 3 Part1-3:2006 (equations (3) and (4)) are compared with pull-out failure experiments on CFS batten screw connections in this section [32-34]. The study also compares the equations established by Mahendran and Tang (equation (5)) [9], and Sivapathasundaram and Mahendran (equation (6)) [10]. The equations developed for ambient temperatures overestimate pull-out capacities at elevated temperatures with a maximum overestimation and underestimation percentage of 59% and -67%, respectively. It is suggested to develop new design rules for pull-out capacities at hot temperatures.

$$P_u = 0.85 t d_f f_u \quad (1)$$

for $t < 0.9$ mm, where t – thickness of sheet not in contact with screw head, d_f – nominal screw fastener diameter ($3.0 < d_f < 7.0$ mm) and f_u – the tensile strength of the sheet not in contact with the screw head in MPa as defined in [35].

$$P_u = 0.85 t d f_u \quad (2)$$

where t – thickness of member not in contact with screw head, d – the nominal screw fastener diameter ($2.03 < d < 6.35$ mm) and f_u – the tensile strength of the member not in contact with screw head or washer as defined in [36].

If $t/p < 1$

$$P_u = 0.45 t d f_u \quad (3)$$

If $t/p > 1$

$$P_u = 0.65 t d f_u \quad (4)$$

where t – thickness of the supporting member into which a screw fastener is fixed, d – nominal diameter of the fastener ($3.0 < d < 8.0$ mm) and f_u – ultimate tensile strength of the supporting member into which a screw fastener is fixed and p - thread pitch.

$$P_u = k d p^{0.2} t^{1.3} f_u \quad (5)$$

where $k = 0.70$ for thinner steel battens made of G250, G500 and G550 steel of thickness $t < 1.5$ mm; $k = 0.80$ for thicker steel purlins and girts made of G450 steel thickness $1.5 < t \leq 3.0$ mm; and $k = 0.75$ for all steel battens and purlins/girts made of G250, G450, G500 and G550 steels of thickness $t \leq 3.0$ mm.

$$P_u = 1.62 k t^{1.3} d^{0.7} f_u [(d-d^*)/p]^{0.3} \quad (6)$$

where $k = 0.88$ for $t < 0.9$ mm high strength steels (G550), 0.96 for $0.9 \text{ mm} \leq t \leq 1.21$ mm high strength steels (G550 and G500), 0.91 for $t \leq 1.21$ mm high strength steels (G550 and G500), 1.07 for $1.21 \text{ mm} < t \leq 2.93$ mm high strength steels (G450) and 1.14 for low strength steels (G250). d^* =larger of d_l or DD , ie. d_l for Zips and T17 screw fasteners and DD for Tek screws.

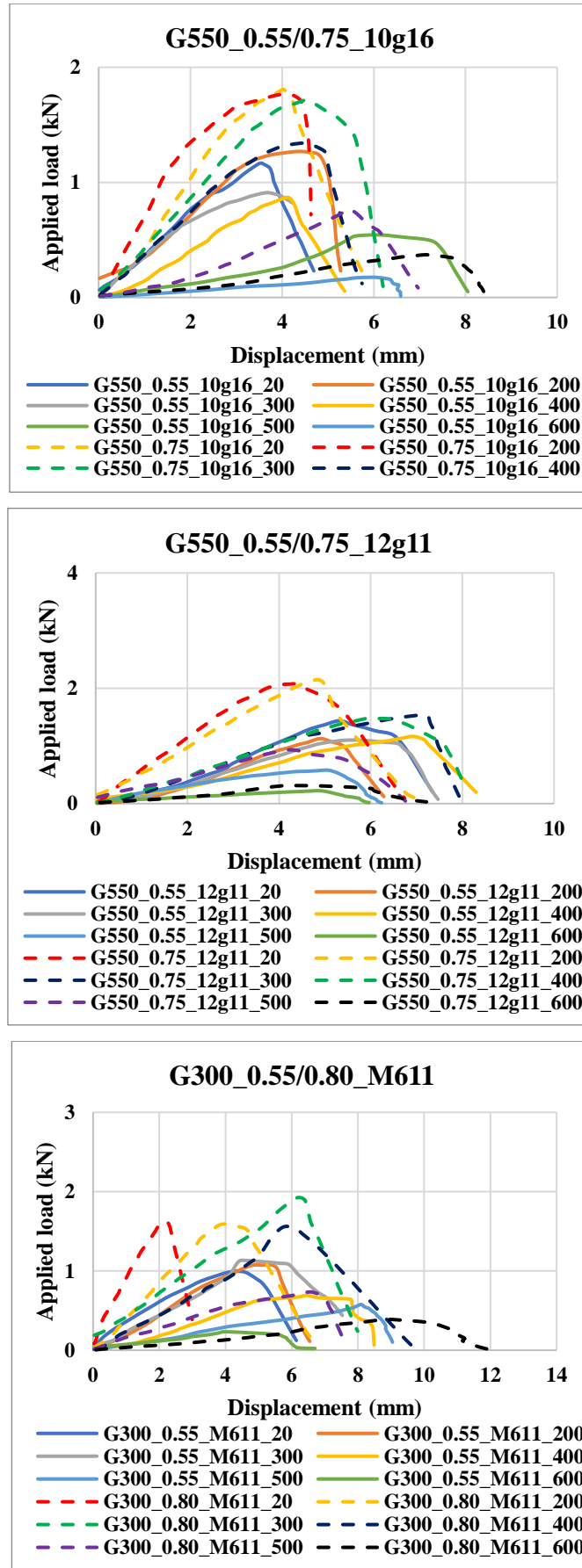


Figure 6: Applied load vs displacement graphs

4.2 New predictive equations

At 600 °C, CFS sheets' Young's modulus decreases about 70% of its ambient value. At ambient temperatures, Young's modulus was not taken into account when calculating batten pull-out capacity. Due to the significant reduction in Young's modulus at 600 °C, new equations are proposed including Young's modulus. Pull-out capacity is determined by parameters such as the thickness of a test specimen, its ultimate tensile strength, the outer diameter of threads, the difference between outer and inner diameters, and the pitch of the threads in the equations (1)-(6). Equation (5) shows an increase in pull-out capacity with increasing pitch size, while others show a decrease. The discrepancy may be caused by omitting thread inner and drill point diameters in equation (5). Screws with smaller pitches will have more threads, resulting in higher load capacity against batten thickness.

In synthetic bone materials, increasing thread pitch reduced pull-out capacity, but decreasing inner diameter increased it [35]. Smaller pilot holes increased capacity, while larger ones resulted in lower failure loads [36, 37]. The pull-out capacity equation was developed taking into account thread pitch, inner diameter and pilot hole size. A curve-fitting method was used to determine batten pull-out capacity at elevated temperatures using dimensionless ratios as illustrated in figure 7. Table 4 shows reasonable agreement between equation (7) and experimental results with $R^2 > 0.95$.

Combined G550 and G300 battens:

$$P_{u,T} = 0.26 t^{1.29} d^{0.71} f_{u,T}^{0.71} E_T^{0.29} [(d-d^*)/p]^{0.29} \quad (7)$$

$P_{u,T}$ –The pull-out capacities at elevated temperatures (N), T -elevated temperatures (°C), t – batten thickness (mm), d –screw outer diameter (mm), $f_{u,T}$ – ultimate strength of CFS at elevated temperatures (MPa), E_T – Young's modulus at elevated temperature. $11 \text{ mm} \leq d \leq 14.5 \text{ mm}$, $0.55 \text{ mm} \leq t \leq 0.75 \text{ mm}$ for G550 battens and $0.55 \text{ mm} \leq t \leq 0.80 \text{ mm}$ for G300 battens. d^* = larger of d_i or DD , ie. d_i for Zips and T17 screw fasteners and DD for Tek screws.

Eqs. (6) and (7) estimate pull-out capacities of battens using t , d , d^* , p , f_u , and T , but show inconsistent coefficients. The COV (0.19) in Table 4 indicates significant variability. Equation (7) with an error margin ranging from -60% to 45% and overestimated by 14.6%. Modifications to equation (8) involves adding a constant (k') to address issues and enhance pull-out capacity predictions. There was an improvement in accuracy (COV- 0.17) with reduced error margins (-46% to 42%) and overestimations (13.5%). Equation (8) outperformed equation (7) significantly in accuracy. At 500 and 600 °C, the pull-out failure loads are lower, and slight deviations from the predictions are more likely to cause a higher error margin to be observed.

$$P_{u,T} = 0.26 k' t^{1.29} d^{0.71} f_{u,T}^{0.71} E_T^{0.29} [(d-d^*)/p]^{0.29} \quad (8)$$

Where, $k' = 0.95$ for G550 battens and 1.09 for G300 battens, rest of them are defined in equation (7).

Table 4: Comparison of experiment and Eq. (7) results at elevated temperatures

Specimen	$P_{u, test}$	$P_{u, test}/P_{u, eq. (7)}$	Specimen	$P_{u, test}$	$P_{u, test}/P_{u, eq. (7)}$
#_0.55_a_20	1165	1.03, 0.85, 1.10	*_0.55_a_20	738	1.03, 0.98, 1.00
#_0.55_a_200	1267	1.12, 1.18, 1.06	*_0.55_a_200	924	1.18, 1.17, 0.95
#_0.55_a_300	1040	1.02, 0.97, 0.89	*_0.55_a_300	855	1.31, 1.13, 1.22
#_0.55_a_400	772	0.93, 1.07, 1.04	*_0.55_a_400	592	1.21, 1.18, 0.99
#_0.55_a_500	584	1.03, 0.88, 0.94	*_0.55_a_500	412	1.30, 1.19, 1.27
#_0.55_a_600	175	0.57, 0.79, 0.59	*_0.55_a_600	147	0.81, 0.71, 0.86
#_0.55_b_20	1439	1.07, 1.06, 1.07	*_0.55_b_20	1146	1.35, 1.33, 1.22
#_0.55_b_200	1126	0.84, 1.08, 0.82	*_0.55_b_200	1306	1.41, 1.25, 1.29
#_0.55_b_300	1127	0.93, 0.92, 0.91	*_0.55_b_300	1158	1.49, 1.60, 1.16
#_0.55_b_400	1174	1.19, 1.18, 0.94	*_0.55_b_400	677	1.17, 1.36, 1.11
#_0.55_b_500	580	0.86, 0.88, 0.88	*_0.55_b_500	435	1.15, 1.16, 1.19
#_0.55_b_600	223	0.61, 0.6, 0.66	*_0.55_b_600	173	0.80, 0.84, 0.86
#_0.55_c_20	1273	0.86, 0.95, 1.05	*_0.55_c_20	997	1.07, 1.01, 1.05
#_0.55_c_200	1386	0.94, 0.87, 0.94	*_0.55_c_200	1075	1.05, 0.99, 1.17
#_0.55_c_300	1161	0.87, 0.89, 0.93	*_0.55_c_300	1141	1.34, 1.31, 1.20
#_0.55_c_400	1061	0.97, 0.90, 0.98	*_0.55_c_400	559	0.88, 0.93, 1.08
#_0.55_c_500	673	0.91, 0.95, 0.79	*_0.55_c_500	435	1.05, 1.09, 1.42
#_0.55_c_600	235	0.59, 0.56, 0.55	*_0.55_c_600	234	0.98, 1.08, 1.04
#_0.75_a_20	1806	1.11, 0.95, 1.07	*_0.80_a_20	1176	1.02, 0.99, 0.98
#_0.75_a_200	1811	1.12, 1.25, 1.24	*_0.80_a_200	1458	1.16, 0.98, 1.15
#_0.75_a_300	1724	1.18, 1.18, 1.17	*_0.80_a_300	1309	1.24, 0.98, 0.97
#_0.75_a_400	1400	1.18, 1.12, 1.16	*_0.80_a_400	946	1.20, 1.19, 1.21
#_0.75_a_500	766	0.95, 1.08, 0.88	*_0.80_a_500	690	1.35, 1.16, 1.20
#_0.75_a_600	350	0.80, 0.80, 0.85	*_0.80_a_600	266	0.91, 0.99, 0.98
#_0.75_b_20	2071	1.08, 1.06, 0.97	*_0.80_b_20	1438	1.05, 0.99, 1.09
#_0.75_b_200	2148	1.12, 1.08, 0.99	*_0.80_b_200	1772	1.19, 1.00, 1.01
#_0.75_b_300	1534	0.89, 0.98, 0.89	*_0.80_b_300	1324	1.06, 0.96, 1.03
#_0.75_b_400	1770	1.25, 1.06, 0.86	*_0.80_b_400	865	0.93, 0.88, 0.91
#_0.75_b_500	823	0.85, 0.98, 0.86	*_0.80_b_500	566	0.93, 1.05, 0.99
#_0.75_b_600	312	0.60, 0.64, 0.60	*_0.80_b_600	249	0.72, 0.69, 0.63
#_0.75_c_20	2146	1.01, 1.03, 0.92	*_0.80_c_20	1629	1.08, 1.00, 1.02
#_0.75_c_200	2068	0.98, 1.09, 1.11	*_0.80_c_200	1599	0.97, 1.17, 1.07
#_0.75_c_300	2044	1.07, 0.89, 1.24	*_0.80_c_300	1922	1.4, 1.36, 1.41
#_0.75_c_400	1506	0.97, 1.03, 1.00	*_0.80_c_400	1206	1.17, 1.12, 1.5
#_0.75_c_500	1101	1.04, 0.77, 0.97	*_0.80_c_500	734	1.1, 0.94, 1.14
#_0.75_c_600	378	0.66, 0.59, 0.71	*_0.80_c_600	390	1.02, 0.94, 0.96
Mean					1.02
COV					0.19

- G550, * - G300, a – 10g-16, b – 12g-11 and c - M6-11.

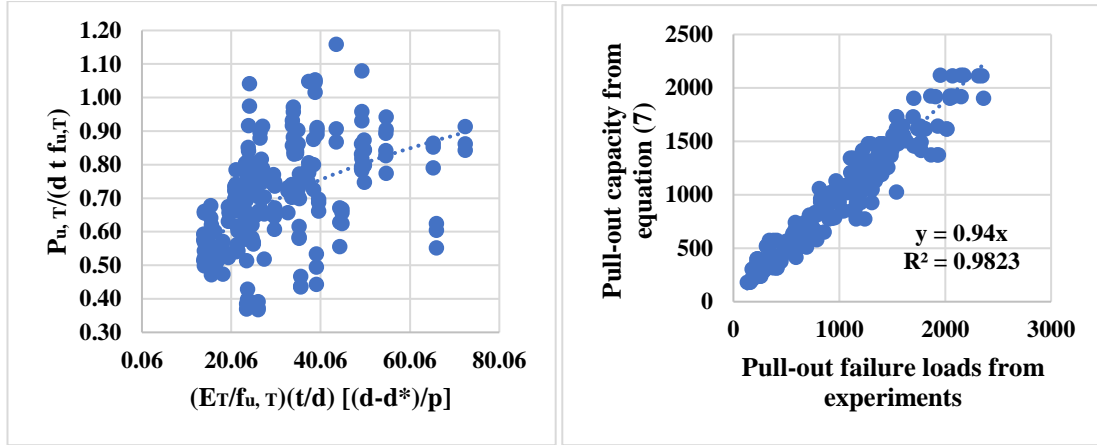


Figure 7: Curve fittings of Predictive Eq. (7) and comparison of Eq.(7) and experiments

5 CAPACITY REDUCTION FACTORS

Design equations from Section 4 determine nominal capacities for battens' pull-out failures. Accuracy entails applying capacity reduction factors to account for material, manufacturing, and test process differences. The equation (9) calculates the capacity reduction factor (ϕ) following the North American standard AISI S100 Chapter K [36]. These measures ensure precise pull-out capacity design under various conditions.

$$\phi = C_{\phi} (M_m F_m P_m) e^{-x} \quad (9)$$

$$x = \beta_o (V_M^2 + V_F^2 + C_F V_P^2 + V_Q^2)^{(1/2)}$$

The P_m , C_P , V_P and ϕ values were determined using the test results for Eqs. (7) and (8), while others were taken from AISI S100 (2016) as shown in Table 5.

Table 5: Capacity reduction factors for new equations at elevated temperatures.

Eq.	Steel grade	M_m	F_m	β_o	V_m	V_F	V_Q	P_m	C_{ϕ}	V_P	n	C_P	ϕ
7	A	1.1	1.0	3.5	0.1	0.1	0.21	1.02	1.52	0.19	216	1.01	0.57
8	A	1.1	1.0	3.5	0.1	0.1	0.21	1.00	1.52	0.17	216	1.01	0.57

A – G550 & G300

At ambient temperature, the capacity reduction factor for pull-out capacities on battens and purlins is 0.55 [10]. There is a reduction factor of 0.55 in equations (7) and (8) for CFS batten pull-out capacities at elevated temperatures.

6 CONCLUSIONS

This study investigated screw connection failure behaviour and capacities under wind uplift and combined bushfire loading. Study results led to formulas for determining thin CFS batten pull-out capacities in such conditions. The pull-out capacities of batten screw connections decreased with increasing temperatures. The design equation (equation (8)) can be used to predict pull-out failure capacities at elevated temperatures. Using numerical studies can help identify the critical parameters that affect pull-out failures at elevated temperatures that experiments can't find. There are still high error margins and detailed solver methods are required to develop more accurate equations.

REFERENCES

- [1] C. Bryant, Understanding bushfire: trends in deliberate vegetation fires in Australia, Technical and background paper series no. 27, Canberra: Australian Institute of Criminology, 2008, <https://www.aic.gov.au/publications/tbp/tbp27>.
- [2] Y. He, K. Kwok, G. Douglas, I. Razali, Numerical investigation of bushfirewind interaction and its impact on building structure, *Fire Saf. Sci.* 10 (2011)1449–1462, <http://dx.doi.org/10.3801/IAFSS.FSS.10-1449>.
- [3] E. Eftekharian, M. Ghodrati, R.H. Ong, Y. He, K. Kwok, CFD investigation of crossflow effects on fire-wind enhancement, in: Proceedings of the 21st Australasian Fluid Mechanics Conference, 2018.
- [4] E. Eftekharian, Y. He, K. Kwok, R.H. Ong, J. Yuan, Investigation of fire-driven cross-wind velocity enhancement, *Int. J. Therm. Sci.* 141 (2019) 84–95, <http://dx.doi.org/10.1016/j.ijthermalsci.2019.03.033>.
- [5] Y. He, Bushfire-wind interaction and its impact on building structure, in: Australian Bushfire Building Conference, 2019.
- [6] M. Slezak,” ‘Almost inconceivable’: 3 billion animals believed killed or displaced in Australia’s summer fires”, ABC News, 2020, <https://www.abc.net.au/news/2020-07-28/3-billion-animals-killed-displaced-in-fires-wwf-study/12497976>.
- [7] Standards Australia, AS 3959: Construction of buildings in bushfire-prone areas, 2018.
- [8] NASH, NASH standard: Steel framed construction in bushfire areas, 2015.
- [9] M. Mahendran, R.B. Tang, Pull-out strength of steel roof and wall cladding systems. *J. Struct. Eng.* 124 (10) (1998) 1192-1201, [https://doi.org/10.1061/\(ASCE\)0733-9445\(1998\)124:10\(1192\)](https://doi.org/10.1061/(ASCE)0733-9445(1998)124:10(1192)).
- [10] M. Sivapathasundaram, M. Mahendran, New pull-out capacity equations for the design of screw fastener connections in steel cladding systems. *Thin-walled Struct.* 122 (2018) 439-451, <https://doi.org/10.1016/j.tws.2017.08.019>.
- [11] M. Sivapathasundaram, M. Mahendran, Pull-out capacity of multiple screw fastener connections in cold-formed steel roof battens. *J. of Const. Steel Research* 144 (2018) 40-52, <https://doi.org/10.1016/j.jcsr.2018.01.013>.
- [12] M. Mahendran and D. Mahaarachchi, Cyclic Pull-Out Strength of Screwed Connections in Steel Roof and Wall Cladding Systems using Thin Steel Battens, *J. Struct. Eng.* 128 (6) (2002) 771-778, [https://doi.org/10.1061/\(ASCE\)0733-9445\(2002\)128:6\(771\)](https://doi.org/10.1061/(ASCE)0733-9445(2002)128:6(771)).
- [13] M. Obeydi, M. Daei, M. Zeynalian, M. Abbasi, Numerical modeling on thin-walled cold-formed steel clip angles subjected to pull-out failures. *Thin-Walled Struct.* 164 (2021), <https://doi.org/10.1016/j.tws.2021.107716>.
- [14] M. Obeydi, I. M. Baltork, M. Zeynalian, Numerical study on the stiffness and ultimate strength of cold-formed steel C-shaped connectors under pull-out failure. *Australian Journal of Struct. Eng.* 24 (2) (2023) 173-189, <https://doi.org/10.1080/13287982.2022.2149977>.
- [15] W. Liu, L. Deng, W. Zhong, Y. Yang, Parametric study on the pull-out performance of screw connections in cold-formed thin-walled steel structures. *Eng. Struct.* 274 (2023), <https://doi.org/10.1016/j.engstruct.2022.115007>.
- [16] S. T. Vy, M. Mahendran, Screwed connections in built-up cold-formed steel members at ambient and elevated temperatures. *J. of Const. Steel Research* 192 (2022) 107218, <https://doi.org/10.1016/j.jcsr.2022.107218>.
- [17] Y. Cai, B. Young, Behavior of cold-formed stainless steel single shear bolted connections at elevated temperatures. *Thin-walled Struct.* 75 (2014) 63-75, <https://doi.org/10.1016/j.tws.2013.10.010>.
- [18] W. Chen, J. Ye, M. Zhao, Steady- and transient-state response of cold-formed steel-to-steel screwed connections at elevated temperatures. *J. of Const. Steel Research* 144 (2018) 13-20, <https://doi.org/10.1016/j.jcsr.2018.01.016>.

- [19] S. Liu, R. Feng, Y. Zhong, Experimental and numerical studies of screwed connections with hot-rolled steel plate and cold-formed steel sheet. *Structures*, 51 (2023) 311-319, <https://doi.org/10.1016/j.istruc.2023.03.063>.
- [20] J. Chen, B. Young, Experimental investigation of cold-formed steel material at elevated temperatures, *Thin-Walled Structures* 45 (1) (2007) 96–110, <http://dx.doi.org/10.1016/j.tws.2006.11.003>.
- [21] T. Ranawaka, M. Mahendran, Experimental study of the mechanical properties of light gauge cold-formed steels at elevated temperatures, *Fire Saf. J.* 44 (2) (2009) 219–229, <http://dx.doi.org/10.1016/j.firesaf.2008.06.006>.
- [22] N.D. Kankanamge, M. Mahendran, Mechanical properties of cold-formed steels at elevated temperatures, *Thin-Walled Struct.* 49 (1) (2011) 26–44, <http://dx.doi.org/10.1016/j.tws.2010.08.004>.
- [23] A. Landesmann, F.C.M. d. Silva, E. d. M. Batista, Experimental investigation of the mechanical properties of ZAR-345 cold-formed steel at elevated temperatures, *Mater. Res.* 17 (4) (2014) 1082–1091, <http://dx.doi.org/10.1590/1516-1439.297014>.
- [24] H.-T. Li, B. Young, Material properties of cold-formed high strength steel at elevated temperatures, *Thin-Walled Struct.* 115 (2017) 289–299, <http://dx.doi.org/10.1016/j.tws.2017.02.019>.
- [25] M. Rokilan, M. Mahendran, Elevated temperature mechanical properties of coldrolled steel sheets and cold-formed steel sections, *J. Constr. Steel Res.* 167 (2020) 105851, <http://dx.doi.org/10.1016/j.jcsr.2019.105851>.
- [26] J. Thistleton, Researchers confirm first 'fire tornado' during 2003 bushfires, *Sydney Morning Her.* (2012) URL <https://www.smh.com.au/environment/researchers-confirm-first-fire-tornado-during-2003-bushfires-20121119-29liv.html>.
- [27] M. Kathekeyan, M. Mahendran, New test and design methods for steel roof battens subject to fatigue pull-through failures. *Thin-Walled Struct.* 119 (2017) 558-571, <https://doi.org/10.1016/j.tws.2017.07.007>.
- [28] European Convention for Construction Steelwork, ECCS TC7 TWG 7.10: Testing of Connections with Mechanical Fasteners in Steel Sheeting, 2009.
- [29] American Iron and Steel Institute, AISI S905: Test Standard for Cold-formed Steel connections, 2013.
- [30] American Iron and Steel Institute, AISI S905: Test methods for mechanically fastened cold-formed steel connections, 2008.
- [31] Standards Australia, AS/NZS 3566.1: Self-drilling Screws for the Building and Construction Industries, Part 1: General Requirements and Mechanical Properties, 2002.
- [32] Standards Australia, AS/NZS 4600: Cold-formed steel structures, 2018.
- [33] American Iron and Steel Institute, AISI S100: North American specification for the design of cold-formed steel structural members, 2016.
- [34] European Committee for Standardization, EN 1993-1-3 (Eurocode 3): Design of steel structures – Part 1-3 General rules – supplementary rules for cold-formed members and sheeting, 2006.
- [35] T.A. DeCoster, D.B. Heetderks, D.J. Downey, J.S. Ferries, W. Jones, Optimising bone screw pull-out force. *J. Orthop. Trauma* 4 (2) (1990) 169–174, <https://doi.org/10.1097/00005131-199004020-00012>.
- [36] H.L.A. Defino, C.R.G. Wichr, A.C. Shimano, F. Kanddziora, The influence of pilot hole diameter on screw pull-out resistance. *Acta Ortop. Bras.* 15 (2) (2007) 76–79.
- [37] B.T. Oktenoglu, L.A. Ferrara, N. Andalkar, A.F. Ozer, A.C. Sarioglu, E.C. Benzel, Effects of hole preparation on screw pull-out resistance and insertional torque: a biomechanical study. *J. Neurosurg.: Spine* 94 (2001) 91–96, <https://doi.org/10.3171/spi.2001.94.1.0091>.